Experimental and Numerical Investigation of Shock Wave-Based Methane Pyrolysis for Clean H_2 Production

Alison M. Ferris, Pujan Biswas, Alka Panda, Luke Zaczek, Rishav Choudhary, Ronald K. Hanson
Department of Mechanical Engineering, Stanford University
Stanford, CA, USA

1 Introduction

With the increasing concern of global CO_2 emissions from fossil fuel combustion, the scientific community is moving towards cleaner, carbon-free fuel alternatives. Hydrogen (H_2), in particular, has been identified as a key fuel that could power next-generation energy systems. However, conventional industrial processes used to produce H_2, including steam methane reforming (SMR) and coal gasification, emit significant quantities of greenhouse gases [1].

Shock-wave reforming, or the use of shock waves to achieve the high-temperature conditions needed to thermally crack a hydrogen-rich feedstock, has emerged as a cleaner alternative that has generated early commercial interest and patented technologies [2–4]. To design and optimize reactors capable of shock wave-based reforming, it is essential to understand the chemical reaction pathways governing this process. Although analysis of the shock-wave reforming process could be extended to a wide variety of energy carriers (e.g., NH_3), the analysis here is limited to thermal pyrolysis of methane as a surrogate for natural gas, as the existing, high-pressure pipeline infrastructure lends itself most readily to the shock-wave reforming approach.

Numerous experimental studies have been carried out to characterize methane pyrolysis behind incident and reflected shock waves (e.g., [5–8]). However, all of the *in situ* kinetics experiments were conducted using highly dilute test gas mixtures, with fuel loading on the order of parts per million (ppm) or 1-5% mole fraction. More recent work probing the pyrolysis of methane/natural gas has started to target higher fuel loading concentrations [9, 10], precisely to determine how product yields may be impacted by initial fuel concentration, and to determine if established kinetic models can accurately capture the fuel-rich reaction kinetics. Even so, there is limited experimental data yet available to evaluate kinetic model performance for methane or natural gas pyrolysis with fuel mole fractions above 10%.

The work presented here has three primary goals: 1) to experimentally measure CH_4 pyrolysis products behind reflected shock waves for previously unexplored, high fuel-loading conditions; 2) to use these results to evaluate kinetic model performance and identify a model capable of accurately simulating fuel-rich CH_4 pyrolysis products; and 3) to exercise the validated kinetic model identified in 2) to better understand the temperature, pressure, and reactor conditions needed to maximize H_2 yields from undiluted CH_4 pyrolysis behind reflected shock waves.

2   Experimental Setup

Fuel-rich, CH_4 pyrolysis experiments were conducted in the Stanford high-purity Kinetics Shock Tube (KST). Laser absorption diagnostics were employed to simultaneously record CH_4, C_2H_2, and C_2H_4 time histories. Chemical-kinetic simulations and prior experimental results [9] indicate that >95% of the initial carbon can be recovered through measurement of these three species, thereby enabling inference of H_2 production through carbon and hydrogen accounting. To measure CH_4, a new diagnostic capable of measuring CH_4 mole fractions spanning 10-40% was developed at a target wavenumber of 3147.63 cm^{-1}. Time-resolved C_2H_4 was measured at 949.49 cm^{-1} (10.532 μm), using a diagnostic previously developed by Ren et al. [11]. C_2H_2 time-histories were measured at 3335.55 cm^{-1} using a diagnostic previously developed by Stranic et al. [12].

3   Results

3.1   Species Measurements & Kinetic Model Evaluation

CH_4, C_2H_2, and C_2H_4 time-histories were recorded for CH_4 pyrolysis experiments spanning 11.5-35.5% CH_4 (mole fraction) in Argon, 1600-2500 K, and 1-4 atm. Figure 1 shows time-history traces for a representative pyrolysis experiment at 2050 K, 3.9 atm (11.5% CH_4/Ar). Chemical-kinetic simulations were also conducted using the CHEMKIN-PRO software package (ANSYS, Inc.) [13]; the simulations were performed assuming constant-internal energy (U), constant-volume (V) constraints and three kinetic models were chosen for comparison: FFCM-1 [14], Aramco 3.0 [15], and PolyMech [16].
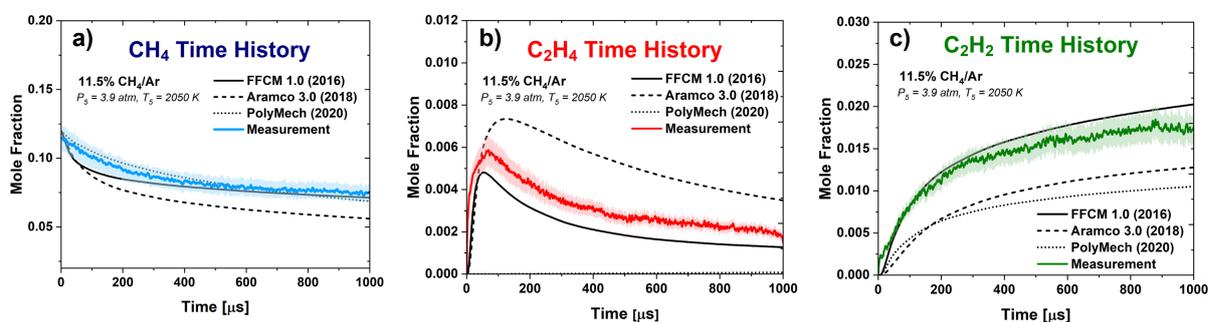

Figure 1: Representative species time-history measurements: 11.5% CH_4/Ar, 2050 K, 3.9 atm.

As can be seen in Figures 1a-c, CH_4 mole fraction decays by ∼35% over the 1 millisecond of reaction time, and most of this decomposition occurs over the first 400 μs. The C_2H_4 time-history indicates rapid production of C_2H_4 in the first 100 μs, followed by rapid decay over the subsequent reaction time. The decay in C_2H_4 is accompanied by a rise in C_2H_2 production, as seen in Figure 1c. Across all three mole fraction time-history plots, the rate of change of each species mole fraction plateaus after approximately 400 μs. This trend can be explained by the endothermicity of the methane pyrolysis process – as endothermic initiation reactions progress, temperature rapidly decreases, leading to a slowing of reaction chemistry, thereby hindering decomposition of CH_4.

Simulated chemical-kinetic model results are also shown in Figures 1a-c. Aramco 3.0 overpredicts the rate and extent of CH_4 decomposition; the model subsequently overpredicts the formation of C_2H_4, leading to the underprediction of C_2H_2 formation. PolyMech captures the experimental CH_4 decay reasonably well, but shows no C_2H_4 formation and significantly underpredicts C_2H_2 formation. Meanwhile, FFCM-1 is able to predict the CH_4, C_2H_4, and C_2H_2 time-histories with reasonable accuracy.

Experiments were additionally conducted with 25.5% CH$_4$/Ar fuel loading. Figure 2 shows species time histories recorded for a temperature sweep of 1619-2410 K at ~3 atm. At the lowest temperature (1619 K), CH$_4$ decomposition is minimal. As temperature is increased, the rate of initial CH$_4$ decomposition increases; the rate of initial C$_2$H$_4$ production and subsequent decay increases concurrently. C$_2$H$_2$ production increases with increasing temperature, as expected.
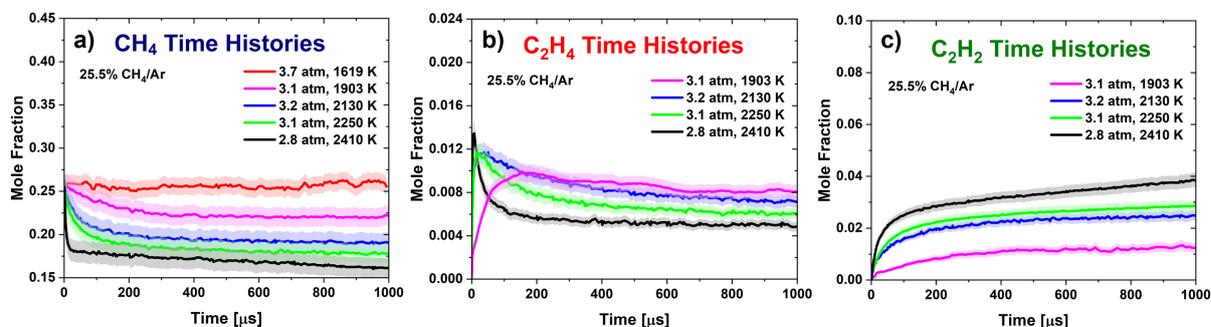

Figure 2: Species time-histories for pyrolysis of 25.5% CH$_4$/Ar (1619-2410 K, 3 atm).

At the highest temperature explored (2410 K), 36.3% of the initial CH$_4$ is consumed over the 1-ms reaction time; recall that in the 11.5% CH$_4$ pyrolysis experiment (2050 K) shown in Figure 1, 35% of the initial CH$_4$ is consumed over 1 ms. The extent of CH$_4$ decomposition is temperature-dependent, therefore the comparison between the 11.5% CH$_4$ and the 25.5% CH$_4$ experiments suggests that for a given reaction time, as fuel loading increases, CH$_4$ decomposition decreases. This observation is consistent with our understanding of the system's endothermicity – when the reactant (CH$_4$) is highly dilute in an inert gas (e.g., Ar), the bulk system temperature is minimally affected by the endothermic pyrolysis process. However, when the reactant is a significant fraction of the total mixture, the bulk system temperature decreases, and this temperature decrease becomes more severe as the initial mole fraction of reactant is increased.

Through the simultaneous measurement of CH$_4$, C$_2$H$_2$, and C$_2$H$_4$, carbon and hydrogen accounting can be performed to infer H$_2$ production. The effectiveness of the thermal pyrolysis process can be quantified through the calculation of a hydrogen yield, defined here as the fraction of hydrogen present in the initial CH$_4$ that is converted into H$_2$: $H_2\ Yield(t) = \frac{N_{H_2}(t)}{2 \times N_{CH_4,init}}$. Here, $N_{H_2}(t)$ is the number of moles of H$_2$ present in the system at time, t, and $N_{CH_4,init}$ is the number of moles of CH$_4$ initially present in the reacting system. A yield of 100%, for example, indicates that 100% of the hydrogen initially present in CH$_4$ has been converted to H$_2$.

Figure 3 shows H$_2$ yields, measured after 1 ms of reaction time, for three fuel loading conditions: 11.5%, 25.5%, and 35.5% CH$_4$/Ar. Kinetic model predictions are included for comparison. As expected, H$_2$ yield increases with increasing initial temperature. H$_2$ yield is also seen to decrease with increasing CH$_4$ loading. The kinetic model results show varying degrees of agreement with the experimental results. Nevertheless, the FFCM-1 kinetic model is found to agree with the experimental results (within the 15-20% uncertainty) for the greatest number of data points.

The measurements presented here represent the first *in situ*, multi-species measurements of CH$_4$ pyrolysis products in a shock tube for fuel loadings greater than 10% CH$_4$/Ar. Comparisons with kinetic models indicate that FFCM-1 predictions agree reasonably well with the experimental results across multiple fuel-loading conditions and temperatures. For the purpose of pyrolysis-driven fuel synthesis, dilute reaction processes are not practical – use of a diluent such as Ar would require energy-intensive separation after the fact, not to mention the extremely low yields that would result from a starting fuel
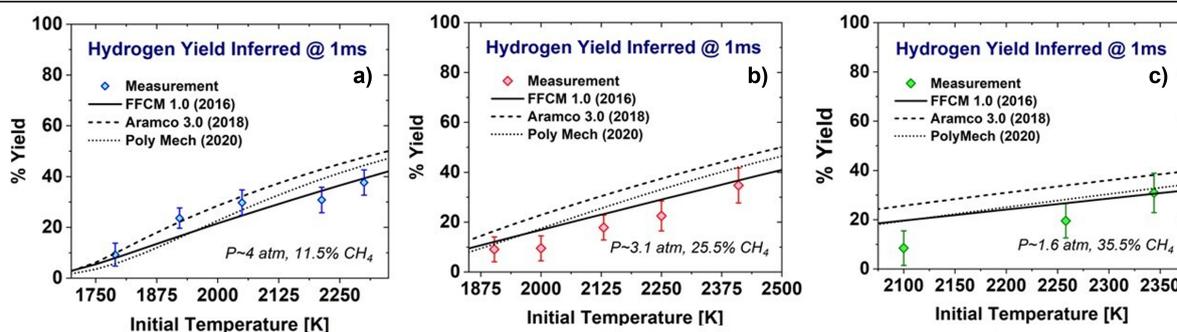
Figure 3: Inferred H$_2$ yields from CH$_4$ pyrolysis (11.5-35.5% CH$_4$/Ar, ~1750-2410 K, 1.4-4 atm).

concentration of 35% or less. It is therefore of interest to understand expected CH$_4$ pyrolysis yields in the absence of a diluent. Analysis of 100% CH$_4$ pyrolysis will therefore be the focus of the next section.

3.2   Kinetic Modeling of H$_2$ Production from 100% CH$_4$ Pyrolysis

Chemical-kinetic simulations were performed to investigate the thermal pyrolysis of 100% CH$_4$ across a wide range of temperature and pressure conditions (1400-2600 K, 1-30 atm). The kinetic simulations were carried out as described above, using the FFCM-1 kinetic model. The FFCM-1 model was chosen for this analysis because of its demonstrated ability to accurately predict the gas-phase product species related to methane pyrolysis (see above). For these initial simulations, a 0-D, constant-internal energy/constant-volume (constant-UV) reactor was assumed – an assumption commonly deployed in the simulation of shock-tube kinetics experiments.
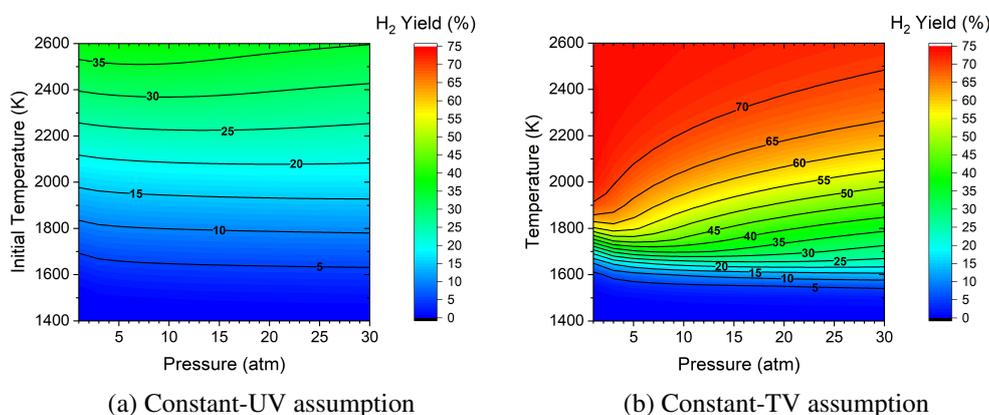

(a) Constant-UV assumption   (b) Constant-TV assumption

Figure 4:   Simulated H$_2$ yields for high-temperature pyrolysis of 100% CH$_4$, assuming a 0-D, (a) constant-UV reactor, (b) constant-TV reactor, and 5 ms reaction time.

Figure 4a shows simulated H$_2$ yields after 5 ms of reaction time from the pyrolysis of 100% CH$_4$. From this plot, it is apparent that H$_2$ yield has a strong dependence on initial temperature, but a weak dependence on pressure. This contour plot also indicates that when the system is subject to constant-UV constraints, the maximum hydrogen yield achievable within 5 ms of reaction time is approximately 37%; as shown in Figures 1 and 2, the rest of the hydrogen is primarily tied up in C$_2$H$_4$ and C$_2$H$_2$. While a yield of 37% is respectable, this value falls short of the hydrogen yields achievable using alternative H$_2$ production technologies.

To better understand how reactor assumptions impact anticipated H$_2$ yields, chemical-kinetic simulations were also performed to investigate the isothermal pyrolysis of 100% CH$_4$ across the same range of temperature and pressure conditions investigated in the constant-UV analysis presented above (1400-2600 K, 1-30 atm). This time, however, a 0-D, constant-temperature/constant-volume (constant-TV) reactor assumption was employed. Forcing the system to maintain a constant temperature (in effect, forcing it to counteract the pyrolysis-driven temperature drop) is expected to provide insight into how a shock-driven system could be modified to maximize hydrogen yields. Figure 4b shows simulated isothermal H$_2$ yields at 5 ms across the full range of relevant temperatures and pressures. It is immediately apparent that the isothermal assumption has a significant impact on the extent of CH$_4$ decomposition: a maximum H$_2$ yield of approximately 74% is achievable at temperatures above 1900 K.

Figure 4a and Figure 4b are both instructive for analyzing the shock-wave reforming process. If a commercial shock-wave reforming device is designed to operate in a constant-UV fashion (Figure 4a), kinetic simulations show that within 5 ms, a maximum H$_2$ yield of approximately 35% is achievable at temperatures greater than 2500 K, and this trend is observed across a range of pressures (1-30 atm). A maximum H$_2$ yield of 35%, however, is not competitive with contemporary reforming strategies (e.g., steam methane reforming), and a post-shock catalytic reactor would likely be necessary to boost total H$_2$ production. On the other hand, if a commercial shock-wave reforming device is designed to operate in an isothermal fashion (e.g., constant-TV), kinetic simulations show that within 5 ms, a maximum H$_2$ yield of 74% is achievable at temperatures as low as 1900 K (Figure 4b). The isothermal H$_2$ yields show a relatively strong pressure dependence, suggesting preferential yields at lower pressures ($<\sim$5 atm).

4   Conclusions

This paper presents a chemical-kinetic analysis of high-temperature, fuel-rich methane pyrolysis, especially as it applies to the concept of shock-wave reforming. A suite of laser absorption diagnostics was used to measure CH$_4$, C$_2$H$_2$, and C$_2$H$_4$ time-histories during CH$_4$ pyrolysis experiments conducted in a shock tube. CH$_4$ pyrolysis was explored across a range of temperature (1600-2500 K), pressure (1-4 atm), and fuel-loading conditions (11.5-35.5% CH$_4$/Ar). Measurements were compared to kinetic model simulations and the FFCM-1 kinetic model was found to predict species time-histories that were consistent with the observed experimental results. Subsequent kinetic modeling showed that when reforming 100% CH$_4$, a maximum H$_2$ yield of $\sim$37% is likely achievable in shock-driven reactors subject to constant-UV constraints, while H$_2$ yields of up to $\sim$74% can be achieved in isothermal reactors. This work provides the first *in situ*, multi-species measurements in fuel-rich ($>$10%) CH$_4$ pyrolysis and provides unique targets for kinetic model refinement.

5   Acknowledgements

References

[1] H. Ishaq, I. Dincer, and C. Crawford, "A review on hydrogen production and utilization: Challenges and opportunities," *Int. J. Hydrogen Energy*, vol. 47, no. 62, pp. 26 238–26 264, 2022.

[2] P. Akbari, C. D. Copeland, S. Tuchler, M. Davidson, and S. V. Mahmoodi-Jezeh, "Shock wave heating: a novel method for low-cost hydrogen production," in *Proceedings of ASME 2021 International Mechanical Engineering Congress and Exposition (IMECE2021)*, vol. 8a. American Society of Mechanical Engineers, 2021, Paper number: IMECE2021-69775.

[3] "New Wave Hydrogen, Inc." https://www.newwaveh2.com, Accessed: 2022-12-11.

[4] "Ekona Power, Inc." https://www.ekonapower.com, Accessed: 2022-12-11.

[5] M. J. Rabinowitz, J. W. Sutherland, P. M. Patterson, and R. B. Klemm, "Direct rate constant measurements for atomic hydrogen + methane → methyl + hydrogen, 897-1729 K, using the flash photolysis-shock tube technique," *J. Phys. Chem.*, vol. 95, no. 2, pp. 674–681, 1991.

[6] D. Davidson, M. Di Rosa, A. Chang, R. Hanson, and C. Bowman, "A shock tube study of methane decomposition using laser absorption by CH_3," *Symp. (Int.) Combust.*, vol. 24, pp. 589–596, 1992.

[7] R. B. Klemm, J. W. Sutherland, M. J. Rabinowitz, P. M. Patterson, J. M. Quartemont, and W. Tao, "Shock tube kinetic study of methane dissociation: $1726 \, K \leq T \leq 2134 \, K$," *J. Phys. Chem.*, vol. 96, no. 4, pp. 1786–1793, 1992.

[8] Y. Hidaka, K. Sato, Y. Henmi, H. Tanaka, and K. Inami, "Shock-tube and modeling study of methane pyrolysis and oxidation," *Combust. Flame*, vol. 118, no. 3, pp. 340–358, 1999.

[9] D. Nativel, B. Shu, J. Herzler, M. Fikri, and C. Schulz, "Shock-tube study of methane pyrolysis in the context of energy-storage processes," *Proc. Combust. Inst.*, vol. 37, no. 1, pp. 197–204, 2019.

[10] J. Shao, A. M. Ferris, R. Choudhary, S. J. Cassady, D. F. Davidson, and R. K. Hanson, "Shock-induced ignition and pyrolysis of high-pressure methane and natural gas mixtures," *Combust. Flame*, vol. 221, pp. 364–370, 2020.

[11] W. Ren, D. F. Davidson, and R. K. Hanson, "IR laser absorption diagnostic for C_2H_4 in shock tube kinetics studies," *Int. J. Chem. Kinet.*, vol. 44, no. 6, pp. 423–432, 2012.

[12] I. Stranic and R. K. Hanson, "Laser absorption diagnostic for measuring acetylene concentrations in shock tubes," *J. Quant. Spectrosc. Radiat.*, vol. 142, pp. 58–65, 2014.

[13] CHEMKIN-PRO 15172, Reaction Design: San Diego, 2016.

[14] G. Smith, Y. Tao, and H. Wang, "Foundational Fuel Chemistry Model Version 1.0 (FFCM-1)," http://nanoenergy.stanford.edu/ffcm1, 2016.

[15] C.-W. Zhou, Y. Li, U. Burke, C. Banyon, K. P. Somers, S. Ding, S. Khan, J. W. Hargis, T. Sikes, O. Mathieu, E. L. Petersen, M. AlAbbad, A. Farooq, Y. Pan, Y. Zhang, Z. Huang, J. Lopez, Z. Loparo, S. S. Vasu, and H. J. Curran, "An experimental and chemical kinetic modeling study of 1,3-butadiene combustion: Ignition delay time and laminar flame speed measurements," *Combust. Flame*, vol. 197, pp. 423–438, 2018.

[16] S. Porras, D. Kaczmarek, J. Herzler, S. Drost, M. Werler, T. Kasper, M. Fikri, R. Schießl, B. Atakan, C. Schulz, and U. Maas, "An experimental and modeling study on the reactivity of extremely fuel-rich methane/dimethyl ether mixtures," *Combust. Flame*, vol. 212, pp. 107–122, 2020.